Turk J Phys
27 (2003) , 145 – 152.
© TÜBİTAK

Electrical Characteristics of Si Doped with Sb by Laser Annealing

Raid A. ISMAIL, Aseel A. HADI
Department of Applied Sciences, University of Technology Baghdad-IRAQ

Received 02.06.2000

Abstract

Laser induced diffusion of antimony in silicon was obtained using a Nd:YAG pulsed laser. The irradiation of antimony-coated silicon by laser beam allowed melting and diffusion of antimony inside the silicon. Diodes were fabricated. Laser beam energy and substrate temperature played a major role in electrical sheet conductivity I-V, and C-V characteristics of the fabricated diodes. High laser energy reduced the electrical sheet conductivity and dominated the recombination current due to the generation-recombination process and trapping centers. On the other hand, the diffusion current dominated for diodes fabricated under heating conditions of the sample during laser irradiation. The C-V measurements of fabricated diodes revealed that the junction were of abrupt type.

Key Words: Laser annealing, LID doping, Silicon devices, Sb dopants

1. Introduction

In recent decades, scientific efforts have led to an expansion of laser applications, especially, in the use of pulsed and continuous lasers in electronic industries, aiming for and leading to components of smaller and smaller dimension that couldn't be achieved by conventional means.

In this respect, the use of lasers follows the final goal of such use. Some scientists employed the laser for scribing and drilling [1,2] of semiconductor wafers, in addition to the annealing processes that frequently follows ion implantation to remove defects [3]. Others scientist have used the laser to induce impurity diffusion in silicon to manufacture p-n junctions and solar cells [4-6].

In this work, electrical sheet conductivity, I-V and C-V investigations of Sb-pSi diodes fabricated by free running pulsed Nd:YAG laser under various conditions are presented.

2. Experimental Work

Single crystal (111) Boron-doped (p-type) silicon wafers of 5Ω· cm electrical resistivity were cleaned by warm distilled water and then washed by ethanol in an ultrasonic bath for 10 minutes. This was followed by chemical etching using a mixture of CH_3COOH, $HNO_3$and HF at 2:3:2 ratio and concentrations of 99%, 70% and 49%, respectively, for 4 minutes. The wafers were washed again with a ethanol, dried then coated with a 200Å thick antimony using a thermal resistive technique under pressure down to 10^{-6} Torr. Each wafer was cut into 1×1 cm^2 samples. The samples were then irradiated by laser at varies energies between 0.18-0.36 J using 300 μs TEM_{oo} Nd:YAG laser pulses with beam diameter of 1mm. The samples were located in an evacuated quartz ampoule chamber at 10^{-3}Torr) and were heated at varies temperatures (room temperature, 373, 448, 523 & 598 K). Figure 1 shows the experimental set-up of this work. For large areas (1 cm^2), 40% overlap between laser pulses was used. NaOH etchant was used after laser doping to remove the residual Sb atoms on the Si surface.

Ohmic contacts were established by deposition on the p-side with a 100Å thick gold film using a DC sputtering unit and the donor side with a 1000Å thick aluminum film using thermal evaporation.

3. Results and Discussion

3.1. Electrical sheet conductivity

Knowing the value of the electrical conductivity gives a clear indication of the extent of doping. To achieve this, a four point probe (type FPP5000) was employed. Figure 2 illustrates the electrical sheet conductivity curve for antimony doped silicon as a function of laser energy. It shows two distinct regions: in the first there is a clear increase in conductivity up to 0.28 J of input laser energy, after which the conductivity starts to decrease. Irradiation with energy lower than this value (the melting threshold value) did not induce diffusion of impurity from the liquid phase leading to the generation of structural defects which, in turn reduced the conductivity [7].

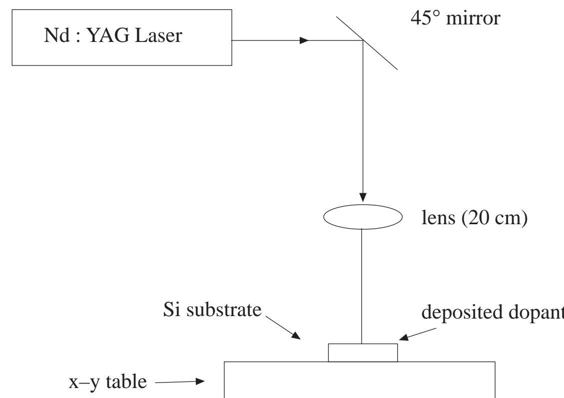

Figure 1. Experimental set-up of laser-induced diffusion.

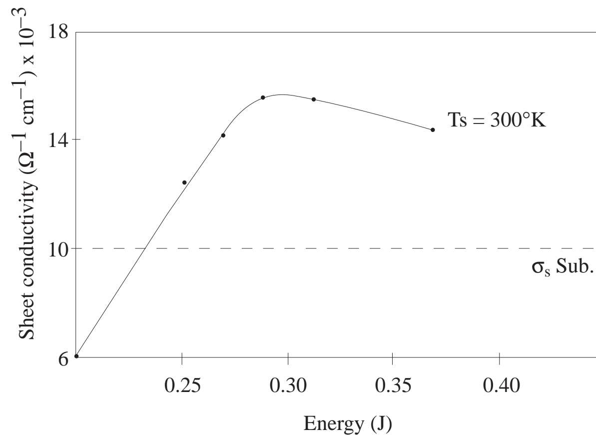

Figure 2. Sheet electrical conductivity versus laser energy.

At the melt threshold value of input laser energy, a substitution of impurity within the silicon lattice took place, resulting in an increase of electrical activity in the doped region [8]. In the second region of Figure 2, the conductivity-laser energy plot flattens (becomes the saturation region). The region contains the highest impurity concentration of heavily doped n^+ [7, 9].

Irradiating with laser energy beyond the melting threshold reduced the conductivity due to the generation and recombination centers which occupy deep energy levels within the energy gap of the silicon (i.e. the ionization energy $> 3KT/q$) [7]. Figure 3 expresses the variation of electrical sheet conductivity with substrate temperature. Heating the sample resulted in an increase in conductivity due to the increase in the melting

depth. Extended depth reduced the solidification rate because of the decrease in the temperature gradient at high substrate temperature [10]. The solidification rate negatively affect the segregation coefficient K phase $K = C_s/C_\ell$, where C_s and C_ℓ are the concentration of doping in solid phase and liquid, respectively. Reduction of the later results in an increase in the substitutional impurity concentration within the under surface region [2] and therefore a growth in the electrical sheet conductivity. Moreover, the temperature rise of the surface reduces the temperature difference of the sample before and after irradiation, which helps reduce the induced defects brought by fast laser heating [11].

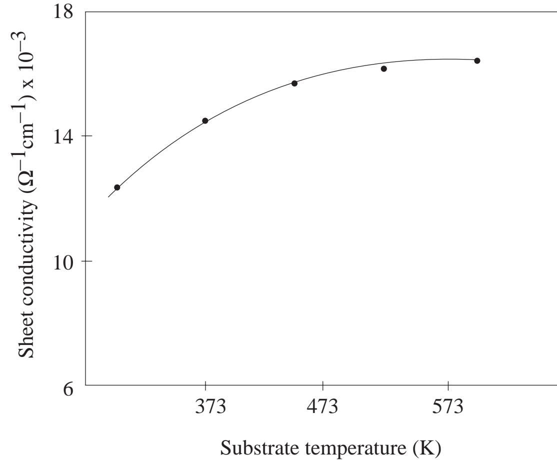

Figure 3. Variation of electrical sheet conductivity with substrate temperature.

3.2. I-V Characteristics

Figure 4 shows the I-V characteristics in forward and reverse bias under dark for antimony-doped silicon using different irradiating laser energies at room temperature.

Figure 4-a shows two regions in the forward current using 0.25 J of laser energy. The first is the recombination current dominated at low bias voltage (lower than $3K_BT/q$). This current is developed because the number of charge carriers generated is greater than that of the intrinsic carrier (n_i), i.e, $n \times p > n_i^2$. To reach equilibrium, there is recombination.

The increase of bias potential to a value greater than $3K_BT/q$ made the forward bias current greater while keeping the recombination current dominant, i.e., no diffusion current existed. After a value of 0.5 V, the biasing current is changing in random manner. This is the series resistance region. Weak I-V characteristics and poor rectification diodes resulted when doped at liquid phase did not result in the domination of recombination current over that of the diffusion. The ideality-factor β representing the efficiency of the diode was 3.2, a value emphasizing the domination of the recombination current. The I-V characteristics at melting threshold 0.288J laser energy express a clear improvement. Figure 4-b points out that the diffusion current in the forward bias dominates for bias value greater than $3K_BT/q$. This behavior fits well with the Shockley equation [12]:

$$I_F = I_{\text{sat}}[\exp qV/(\beta K_BT) - 1] \tag{1}$$

where I_{sat} is the saturation current, q is the electron charge, V is the applied voltage, K_B is the Boltzmann constant, and T is the operating temperature.

Figure 4-b shows also the represents of series resistance (curvature at high voltage) brought about by some defects within the depletion layer. The reverse bias current comprises two regions. The first is the generation current:

$$I_g = Awqn_i/\tau_o, \tag{2}$$

which depends on the bias potential, where A is the diode area, W is the depletion layer width, and τ_o is the carrier lifetime within the depletion layer.

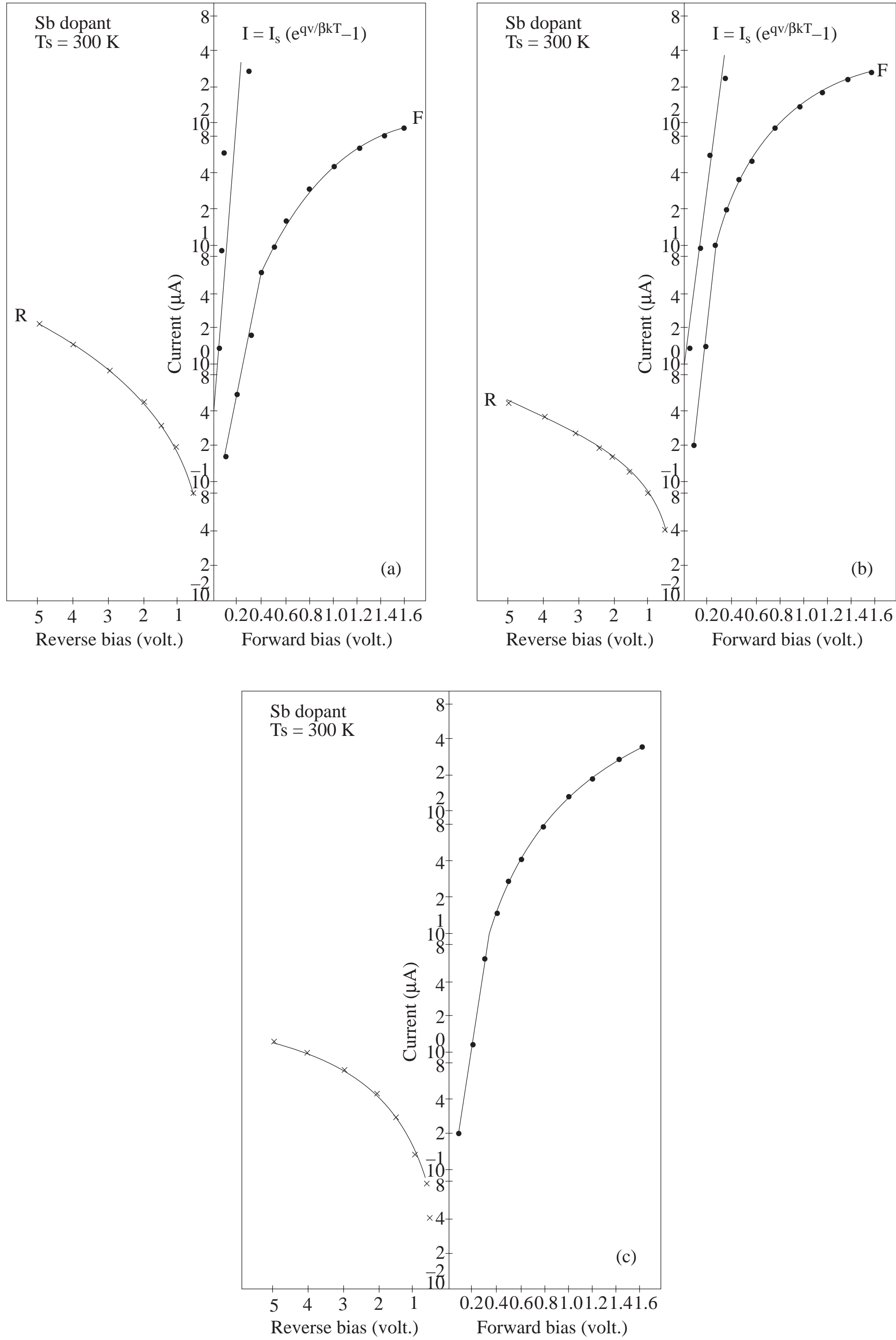

Figure 4. I-V characteristics of p-n Junction diodes fabricated with different laser energies: (a) 0.25 J (b) 0.28 J (c) 0.39 J.

The increase in the biasing potential leads to an increase in W, which in turn increases I_g. After value of 2.5 V of bias potential, the second region developed. Here, the reverse bias current stabilizes and becomes independent of the bias potential. This is called the diffusion current I $_{dif}$ which is given as [12]:

$$I_{dif.} = qA\sqrt{D_h \tau_h} n_i^2 / N_D, \tag{3}$$

where D_h is the diffusion coefficient of minority carriers (holes), N_D is the impurity concentration in the donor side and τ_h is the life time of holes.

Figure 4-c reveals unstable reverse bias current with bias potential resulted from structural defects induced at high laser energy and leading to the soft breakdown. The ideality factor at increased laser energy has increased by 25% over its value at melting threshold; see Figure 5.

The forward and reverse bias current as a function of bias voltage for diodes fabricated with 0.18 J of laser energy (this value is not sufficient to make diffusion of Sb in Si at 300 K) and sample heating to 598 K is plotted in Figure 6. As compared to diodes fabricated at room temperature, good features can be observed due to the reduction of defects. Heating the sample to 523 K caused a reduction in the ideality factor to 1.7; see Figure 7. This is attributed to the improvement in the crystal characteristics induced by heating [13].

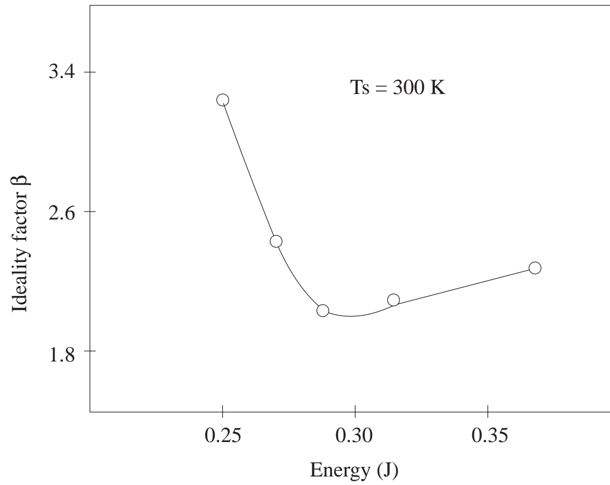

Figure 5. Ideality factor as a function of laser energy.

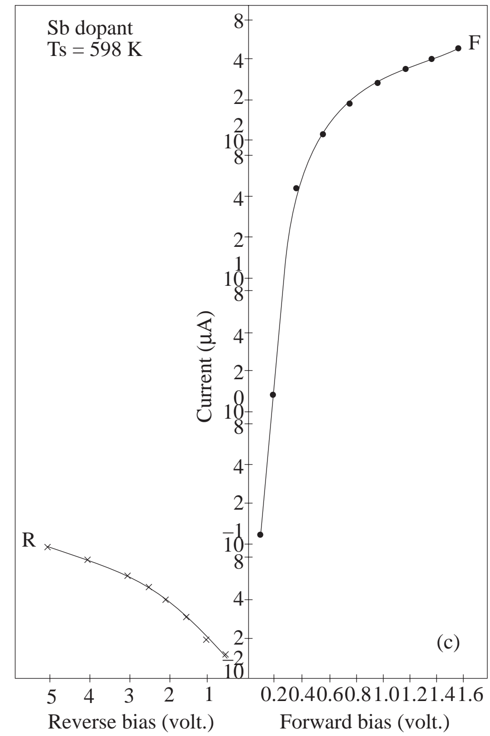

Figure 6. I-V characteristics of diodes fabricated with laser energy 0.18 J and 598 K substrate temperature.

3.3. C-V Chacteristics

Figure 8 is a $1/C^2$ versus V_b plot. The built-in potential V_{bi} was determined from the intersect of curve with the potential axis. It also shows the junction is abrupt [14]. Figure 9 expresses a relation of V_{bi} with irradiating laser energies.

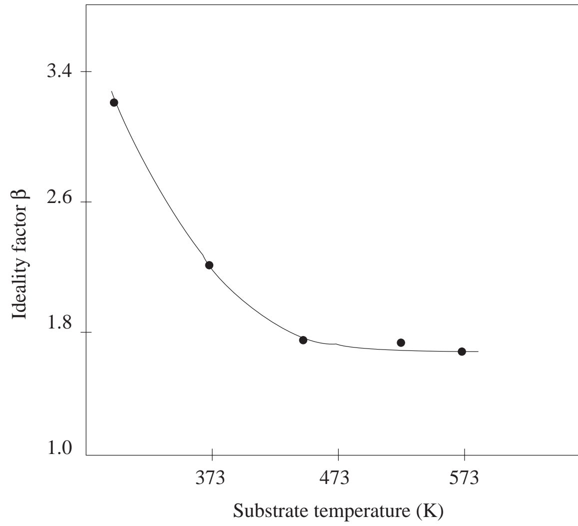

Figure 7. Ideality factor as function of substrate temperature for diodes fabricated with laser energy 0.25 J.

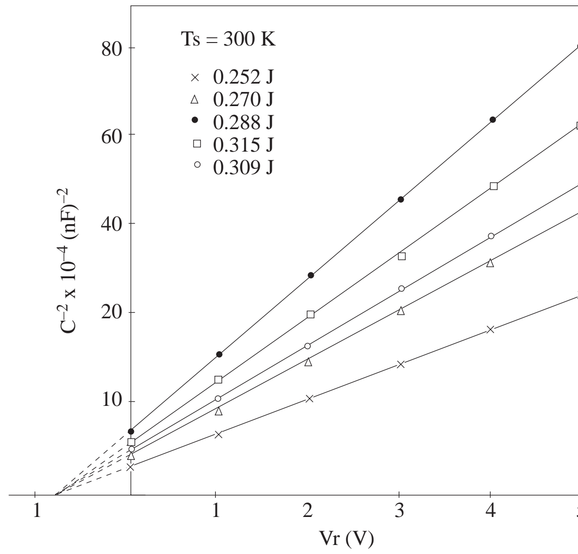

Figure 8. $1/C^2$ versus reverse bias voltage plot for diodes fabricated with different laser energy.

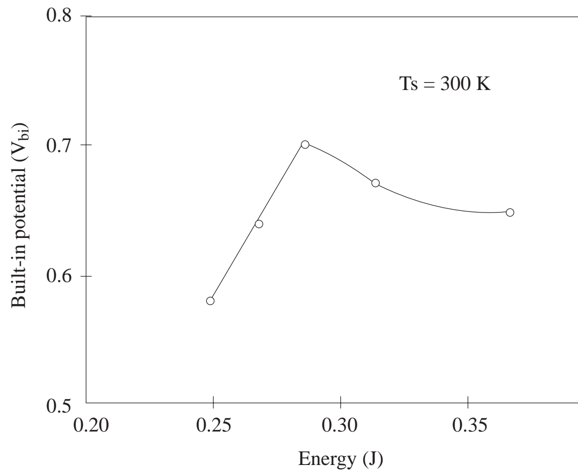

Figure 9. Built-in potential as a function of laser energy for fabricated diodes.

Minimum V_{bi} resulted when using small laser energies. At those energies diffusion from liquid phase did not occur (due to rapid heating and cooling). At melting threshold energy, V_{bi} becomes greater due to the increase in the impurity concentration. The use of energies higher than the melting threshold value caused reduction of V_{bi}. This is due to the defects (induced at high laser energies) which compensate the impurity role [9]. In addition to this, the increase of substrate temperature helped V_{bi} to grow as shown in Figure 10. From the $1/C^2$ versus V plot the substrate concentration was calculated as $4.6 - 6 \times 10^{15}$ cm^{-3}. These values are very close to those obtained from sheet resistance measurements made by four-point probe.

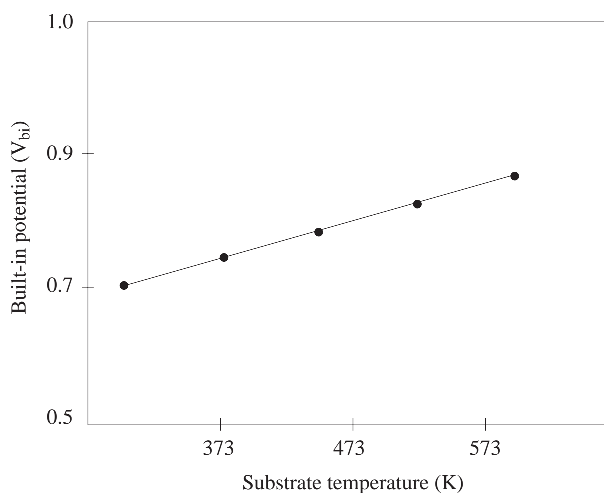

Figure 10. Variation of built-in potential as a function of substrate temperature for diodes fabricated with laser energy of 0.28 J.

4. Conclusions

The results of I-V and C-V for fabricated diodes showed their dependence on Laser energy and substrate temperature. Diffusion of impurity with laser energies lower or greater than the melting threshold value produced diodes with bad characteristics (poor rectification). The best diodes were obtained when using melting threshold laser energy and heating substrate above room temperature. The C-V measurements showed that the fabricated diodes are from the abrupt type.

References

[1] J. F. Ready "Industrial Applications of Laser", (Academic Press, London 1997), 419, 428.

[2] M. Bass, "Laser Material Processing", (North Holland Publishing Company 1983), Ch.7.

[3] K. G. Ibss, M. L. Lloyd, "Ultravoilet Laser Doping of Silicon", *Optics and Laser Technology*, (1983), 35.

[4] A. Mousa and R. A. Ismail, "P-N Junction Formation in Germanium Dipped Into $Al_2(So_4)_3$ Solution by Laser Irradiation", *Engineering and Technology*, **15(1)**, (1996).

[5] D.L. Hansen, B. R. Lehere, W.M., "Development of a Multi-Purpose, Pulsed Laser System for Solar Cell Processing Applications", conference record of the IEEE photovoltaic specialists conference Vol.1, Published By IEEE USA. (1990), 278-283.

[6] J. Narayan, "Laser Processing of Materials", *J. of Materials*, (1980), 18.

[7] V.C. Lo, Y. W. Wong, "Excimer Laser Assisted Spin-On Doping of Boron into Silicon", *Semicond. Sci. Technol.*, **11** (1996), 1285.

[8] W.L. Brown, "Unique Semiconductor Materials and Structures Produced by Laser and Electron Beam", *J. Vac. Sci. Technol.*, **20(1)**, (1982), 734.

[9] E.A. Al-Nuaimy and J. M. Marshall, "Exciemer Laser Crystallization and Doping of Source and Drain Regions in High Quality Amorphous Silicon Thin Film Transistor", *Appl. Phys. Lett.*, **69(25)**, (1996), 3857.

[10] J. Narayan, "Development of morphological instability and formation of cells in silicon alloys during pulsed laser irradiation", *J. of Crystal Growth*, **59**, (1982), 583.

[11] G.J. Galvin, J. W. Mayer, and M. O. Thompson, "Layered Structures and Interface", Ed's Furukawa, KTK Scientific publishers, Tokyo, (1985), 3.

[12] S.M. Sze, "Semiconductor Devices: Physics and Technology", (John-Wiley and Sons, New York 1985).

[13] A. Slaoui, F. Foulon, and M. Blanconi, "Laser and Particle Beam Chemical Processes on Surface", Ed's A. Wayane, G. L. Loper and T. W. Singmon, "Boron Doping of Silicon Using Excimer Lasers", *Mat. Res. Soc. Symp. Proc.*, **129**, (1989), 591.

[14] D.A. Vakhabor, A.S. Zakiror "Feasibility of Fabrication of P-N Junction in Silicon by Millisecond Laser Radiation Pulses", *Sov. Phys. Semicon.*, **15(4)**. (1981), 455.